IEEE Photonics Journal
An IEEE Photonics Society Publication

Open Access

Transmitters for Combined Radio Over a Fiber and Outdoor Millimeter-Wave System at 25 GHz

Volume 12, Number 3, June 2020

Jan Bohata, *Member, IEEE*
Matej Komanec
Jan Spacil
Radan Slavik, *Senior Member, IEEE*
Stanislav Zvanovec, *Senior Member, IEEE*

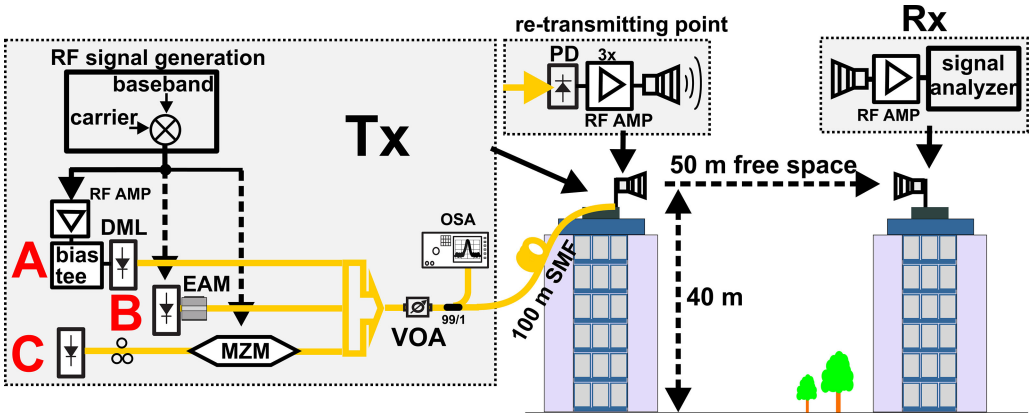

DOI: 10.1109/JPHOT.2020.2997976

Transmitters for Combined Radio Over a Fiber and Outdoor Millimeter-Wave System at 25 GHz

Jan Bohata,[1] ***Member, IEEE***, **Matej Komanec**,[1] **Jan Spacil**,[1]
Radan Slavik,[2] ***Senior Member, IEEE***,
and Stanislav Zvanovec,[1] ***Senior Member, IEEE***

[1]Department of Electromagnetic Field, Faculty of Electrical Engineering, Czech Technical University in Prague, 166 36 Prague, Czech Republic
[2]Optoelectronics Research Centre, Faculty of Engineering and Physical Sciences, University of Southampton, SO17 1BJ Southampton, UK

DOI:10.1109/JPHOT.2020.2997976

Manuscript received April 16, 2020; revised May 20, 2020; accepted May 24, 2020. Date of publication May 27, 2020; date of current version June 22, 2020. This work was supported in part by a project from the Ministry of Industry and Trade in the Czech Republic (FV30427) in part by Grant Agency of the CTU in Prague (SGS20/166/OHK3/3T/13), and in part by COST action CA 16220. Corresponding author: Jan Bohata (e-mail: bohatja2@fel.cvut.cz).

Abstract: In the modern wireless networks, millimeter-wave radio-frequency (RF) bands are becoming more attractive as they provide larger bandwidth and higher data rates than the today-used systems operating at frequencies below 6 GHz. In addition, according to the fact that coaxial cables exhibit extremely high attenuation for millimeter-wave RF signals, analog radio over fiber techniques (RoF) form a promising technology for delivering unaltered radio waveform to a remote antenna. This paper experimentally analyzes three types of RoF modulations, namely a directly modulated laser, an electro-absorption modulator, and a Mach-Zehnder Modulator. The primary focus is on the implementation of each RoF transmitter in an RoF system, such as those in 5G networks. The experimental study includes a detailed characterization of an RoF system with a 50-m long outdoor free-space RF channel operating in the frequency band of 25 GHz. Frequency response (S-parameters) and third-order nonlinear distortion are investigated in detail. Tests of EVM performance were conducted using an orthogonal frequency division multiplexing signal modulated with 16-quadrature amplitude modulation (16-QAM) with a long-term evolution signal. It is demonstrated that the transmitters studied can operate under a 13.5% EVM limit given for 16-QAM. Apart from the detailed system performance, the considerable power fluctuations in the 25 GHz free-space RF outdoor channel are reported.

Index Terms: Microwave photonics, optical fiber, millimeter wave, radio over fiber, optical modulator.

1. Introduction

Global data traffic in wireless networks is increasing exponentially, mainly due to video applications and high-resolution streaming, and it is expected that about 75% of the 69 Exabytes of total worldwide mobile data traffic will be used for video by 2022 [1]. This demand is driving the rapid evolution of wireless technology and incorporates higher frequency bands than those used today to offer significantly greater bandwidth, which is of particular importance for the 5th generation (5G) mobile networks. In addition to higher bandwidths, 5G networks need to deliver latency as low as

1 ms and data rates in the order of tens of Gb/s delivered to a high number of users, e.g., through highly directional beamforming [2].

High-frequency bands for 5G are mostly planned in the millimeter-wave (mm-wave) range of the electromagnetic spectrum. Due to the presence of atmospheric absorption across the mm-wave spectrum and a critical lack of available frequency bands, 24–28 GHz, 37–40 GHz and 64–71 GHz are the best candidates for 5G [2], in particular for smaller cells in cloud radio access network (C-RAN) architecture which tends to centralize the control of remote base stations. In C-RAN networks, radio over fiber (RoF) technology is very likely to be used for mm-wave transfers due to low attenuation and extremely large signal bandwidths [3], [4]. The usage of RoF system for mobile fronthaul networks can be digital or analog. However, especially for 5G networks, the analog RoF implementation helps in shifting of expensive analog-to-digital and digital-to-analog converters to the central office. [5] In the analog RoF approach with direct detection, a radio signal for wireless transmission is modulated onto an optical carrier, propagated via a standard single-mode optical fiber (SSMF) and directly detected by a photodiode keeping the radio frequency (RF) signal in original form, which is ready for antenna transmission. [6]. In this case, the distance between the RoF transmitter and receiver, e.g., for a remote antenna system, can be up to 50 km [7], [8]. Notwithstanding the long distance, RoF technology can operate for upper 5G mm-wave bands as was shown, for example, at 60 GHz for a 2.2-km long RoF link with a laboratory tested 4-m long free-space RF channel with leaky-wave antennas [9]. A comprehensive review of mm-wave frequency RoF systems was provided in [10].

As mentioned, an RoF transmission requires the RF signal to be first modulated on an optical carrier. The most established scheme for high-end RoF links is based on an external modulation performed in a lithium-niobate ($LiNbO_3$) based Mach-Zehnder Modulator (MZM), which is biased in quadrature bias point. Its advantages are large bandwidth ($>$40 GHz), negligible modulation chirp, low insertion loss (IL), low distortion, high power handling, and a relatively high extinction ratio (ER) [6]. Disadvantages include large size, high cost, low output optical power when operating in a linear area resulting in the need for a high power optical source, and low RF-to-optical modulation efficiency. However, the size of MZM can be reduced by integrating, as shown for example in [11]. Note that by using single drive MZM in the null transmission point, a carrier suppressed regime can be achieved, resulting in frequency doubling of the original RF signal after beating in a photodiode, as experimentally demonstrated in laboratory conditions [12], [13]. However, the operation in the null transmission point further reduces optical signal power due to high losses and second MZM needs to be used for data modulation.

The second option for external modulation is to use an electro-absorption modulator (EAM) capable of operating at high frequencies (up to 40 GHz). It is small in size and can be integrated with the laser source [14]. Its disadvantages include a slight modulation chirp, relatively low power handling, and modest ER in a trade-off with modulator losses. [15]

Another option for the RoF transmitter is the direct modulation of a high-bandwidth, directly modulated laser (DML). It represents the simplest and most compact solution as light generation and modulation occur within a single device. Direct modulation offers satisfactory RF to optical conversion efficiency and linearity but has relatively low output power and the modulation chirp is generally higher than the external modulation techniques [16]. A comparison of DML and external modulation using MZM for RoF links has already been presented e.g. in [17] states that MZM type links suffer from relatively high cost and complexity, especially when compared to DML links. Therefore, it seems that DMLs and EAMs are more suitable for microwave/photonic networks thanks to their low price and small size. Another experimental comparison between direct and external modulation at 60 GHz has been presented in [18], however, authors substituted real channel just by a variable attenuator, which cannot fully mimic the free space transmission channel parameters.

Published results on mm-wave transmissions over optical infrastructures mostly report on experiments performed in a laboratory environment. Recently, a 1 Gb/s full-duplex transmission using a silicon ring modulator and integrated III-V photodiode with downstream/upstream carriers at 15/11.5 GHz was presented in [19]. In [20] a DML transmission of 1 Gb/s RoF at 24 GHz over a

50-m long SSMF was demonstrated. To compensate for losses in the optical link, an erbium-doped fiber amplifier (EDFA) was used. Although error vector magnitude (EVM) was as low as 3.4% at the carrier frequency of 3.5 GHz, it was unacceptably high (20.5%) at 24 GHz when using quadrature phase-shift keying modulation. In [21], a 28 GHz 5G RoF system, using universally filtered orthogonal frequency division multiplexing with optical heterodyning, was presented. It used externally injected gain-switched distributed feedback laser realizing transmission over 25 km of SSMF and a 10-cm free-space RF channel with Vivaldi antennas. The total aggregated data rate was 4.56 Gb/s. In [22], the photonic generation of an RF multiple-input-multiple-output signal, in a dense wavelength division multiplexing RoF setup with MZMs, has been described and a 1 Gb/s transmission through 2 km of RoF, and an additional 6-m free-space RF channel was demonstrated. Another published work showed an experimental long-term evolution (LTE) transmission in a multi-service RoF system at 26 GHz [23]. This demonstration contained a 0.75-m long indoor RF channel and achieved 8% of EVM with 64-quadrature amplitude modulation (64-QAM), 10 MHz bandwidth, and an SNR of 30 dB. An RoF transmission over 20 km of SSMF and 10 m long RF free space channel including photonic mm-wave generation at 60 GHz for 5G fronthaul using MZM was presented in [24]. A microwave photonic link using the combination of free space optics (FSO) and 1 m long RF wireless channel operating at a frequency of 28 GHz was shown in [25] [26]. In addition, our previously published work [27] showed the most detailed experimental demonstration of RoF using DML that includes radio over free-space optics and a 3.3 m long indoor wireless free-space RF channel in the frequency band of 24–26 GHz.

Several papers reporting on an outdoor free-space RF transmission within RoF system have been also published. A 60 GHz RF transmission over a combined optic link for broadband photonic transmission wireless links was realized in [28] using self-pulsating mode-locked lasers and high output power photodetectors. In this case, two setups using EAM and MZM were demonstrated for the testing of an outdoor RF transmission for distances up to 25 m. Another report showed the possible integration of a W-band RoF link with passive optical networks [29]. For this purpose, a common, small, form-factor pluggable laser module was used for a 2.5 Gb/s transmission over 15 km of SSMF and an up to 225-m long free-space RF channel with parabolic antennas at a W-band frequency of 86 GHz. However, none of these outdoor experiments was carried out at the 25 GHz mm-wave band, which is the most probable spectral band to be adopted in early 5G and future wireless networks.

In this paper, we present experimental results from a mm-wave RoF outdoor system with a free-space RF channel operating in the 25 GHz band. We analyze the implementation of three transmitter topologies, including MZM, EAM and DML. The proposed transmission scheme and the environment represent real RoF deployment in an urban scenario for transmitting a wideband signal. The paper is organized as follows: The experimental setup is described in Section II, results from the indoor and outdoor measurements are presented in Section III and IV, respectively, a discussion is given in Section V and finally, the summary is provided in Section V.

2. Experimental Setup

At first, we performed an indoor measurement whose laboratory scheme is shown in Fig. 1. To emulate real data transmission format, the RF signal was composed of a baseband (BB) signal containing an orthogonal frequency division multiplexing (OFDM) LTE evolved universal terrestrial radio access (E-UTRA) test model TM3.2 with 16-QAM used for testing output power dynamic and transmitted signal quality [30]. The 20-MHz wide LTE bandwidth was generated by an R&S SMW200A signal generator and up-converted into an RF modulator (RF-MOD) by a 25 GHz single-tone carrier frequency provided by another signal generator R&S SMF100A. It resulted in output power of -10 dBm in the given signal bandwidth. Subsequently, the RF signal was modulated onto an optical carrier using three transmitter modulation techniques with particular parameters given in Tab. 1.

Note that mm-wave generation, providing high-quality signal with low phase noise, can also be realized in the optical domain as was shown e.g. in [4] and [28].

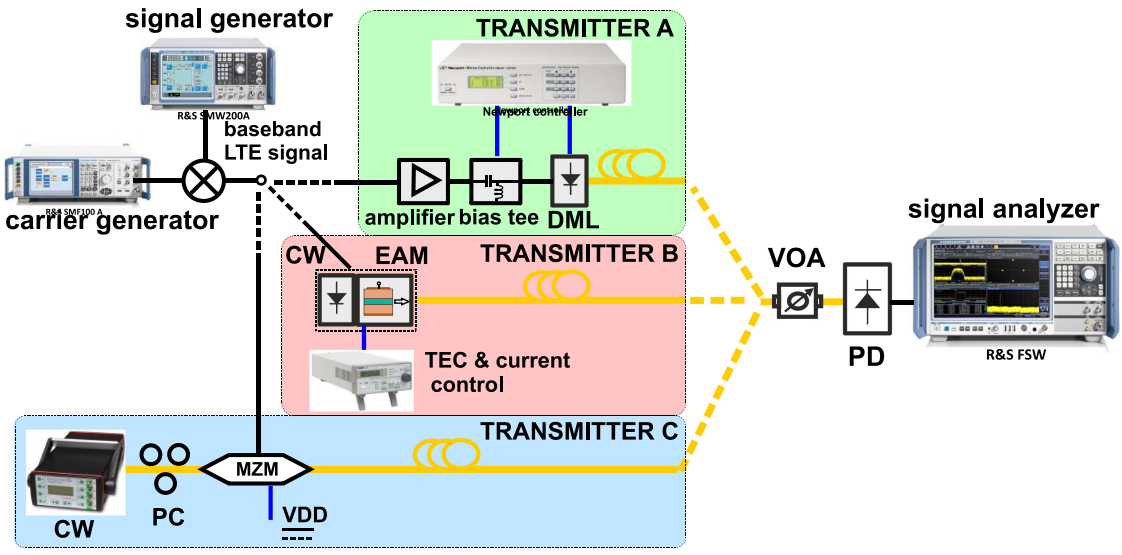

Fig. 1. Indoor laboratory set-up in which Transmitter A, B, or C is used.

TABLE 1
Comparison of Selected Transmitters Parameters

Transmitter	Employed scheme	Modulation bandwidth -3 dB (GHz)	Optical output power (dBm)	side-mode suppression ratio (dB)	Static extinction ratio (dB)
Transmitter A	DML	≥ 35	≥ 1.6	≥ 50	≥ 30
Transmitter B	EAM	≥ 32 GHz	6.7	≥ 35	≥ 15
Transmitter C	MZM	> 25 GHz	6.6	≥ 40 (external CW laser)	≥ 20

Although we use here only 20 MHz bandwidth, the testbed is examined over larger transmission bandwidth at the target frequency band of 25 GHz with emphasis on the comparison of particular modulation techniques. The DML (manufactured in HHI Berlin, commercially available) employed to form Transmitter A was a monolithically-integrated passive feedback laser [31]. It required a bias-tee (SigTek SB12D2) with bias current control and temperature stabilization (both driven by a Newport 8000 modulator controller). The input RF signal was first amplified by an RF amplifier (Wisewave AGP- 33142325-01) to optimize power at the output of the RoF link. Optical output power (laser bias current of 59 mA and temperature of 35 °C) was 1.6 dBm.

Transmitter B was based on an external EAM (OKI OSC-LDS-EML-C-500C) packaged with a continuous wave (CW) laser in a butterfly assembly. It was of comparable size to the DML, which was also in a butterfly package. The EAM required temperature control (Thorlabs TED200C, set to 35 °C in our experiments) and a bias current (Thorlabs LDC205C) set to 100 mA. Its average optical output power was 6.7 dBm.

Finally, Transmitter C used a CW laser (CoBrite DX4) with an external $LiNbO_3$ 40 Gb/s MZM (Fujitsu FTM7938EZ/201) biased at the quadrature point with optical power of 6.6 dBm at the output of the MZM.

The highest requirement for power consumption of the tested transmitters lay in RF signal generation, which was the same for all transmitters, although Transmitter A used an additional

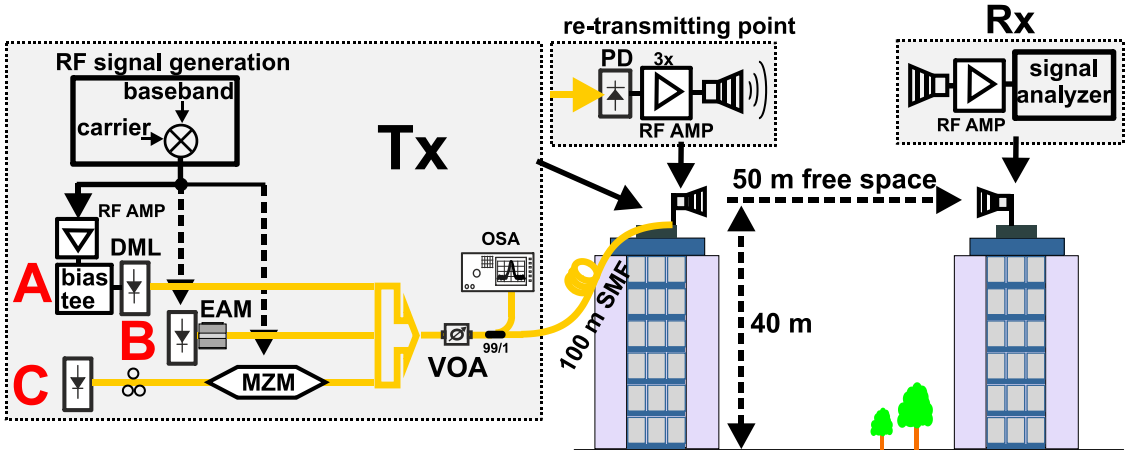

Fig. 2. Outdoor RoF link and 50-m long free-space RF channel. All three transmitters (A, B, and C) are shown. In the experiment, only one transmitter was used at a time.

low noise RF amplifier to compensate bias tee losses. Another power consumption requirement arose from the temperature control, which was however, needed for all laser sources and optical signal generation. The tested optical sources consumed approx. 0.5 W with strictest demands to Transmitter C, which needed to produce the highest optical power, whereas the lowest power consumption had DML in Transmitter A.

The signal from the transmitter under test (A, B, or C) firstly passed through a variable optical attenuator (VOA, Oz optics - DA-100-SC-1300/1550-9/125-S-40 with 1.5 dB of IL) and a 100-m long SSMF. For indoor measurements, the signal was further detected by a photodetector (Optilab PD-40) and analyzed with an R&S FSW signal analyzer.

In the next step, the outdoor setup was proposed to compare indoor and outdoor system performance. Outdoor measurements included a free-space RF channel, which was comprised of two antennas (transmitter antenna - Tx and receiver antenna - Rx) placed on the rooftops of two 9-story building towers, both of which are part of the campus of the Faculty of Electrical Engineering, Czech Technical University in Prague. This enabled 50-m long free-space RF transmission in real atmospheric conditions about 40 m above ground level. The entire setup is shown in Fig. 2, where the 100-m long SSMF between the VOA and the photodetector represented a typical distance of an RoF link, such as what is needed to connect a roof-top antenna with a ground-level central office. Note that the 100-m long SSMF was part of the installed network to mimic a real scenario, e.g. inside a large business building. As will be shown later, SSMF length can be significantly extended without introducing any system performance degradation. To compensate for the relatively large loss of the 50-m long free-space RF channel, the photo-detected signal was amplified with a cascade of three low-noise amplifiers (LNAs) (Miteq AMF-4F-260400-40-10p, Analog devices HMC1131, and Qorvo TGA4536-SM), boosting the power at the transmitting antenna input up to 14.3 dBm. The two RF antennas used to transmit the signal over the free-space RF channel between the buildings (see Fig. 3) were double ridged horn antennas (DRH40–RFspin, s.r.o.) with 14.7 dBi gain at 25 GHz. The free-space loss for antenna transmission at 25 GHz over the 50-m long channel was 94.4 dB, reduced to 65 dB by the antenna gains.

The RF signal received by the receiver antenna was boosted with an LNA (Miteq AMF-4F-260400-40-10p) to compensate for losses of the free-space transmission and the 3-m long coaxial cable (9 dB loss at 24 GHz [32]) connecting the antenna to the signal analyzer. Note that the additional internal amplifier of the signal analyzer was used for Transmitter A enabling the incoming signal, which was weaker in the case of Transmitter A, to set a comparable power level for all three transmitters.

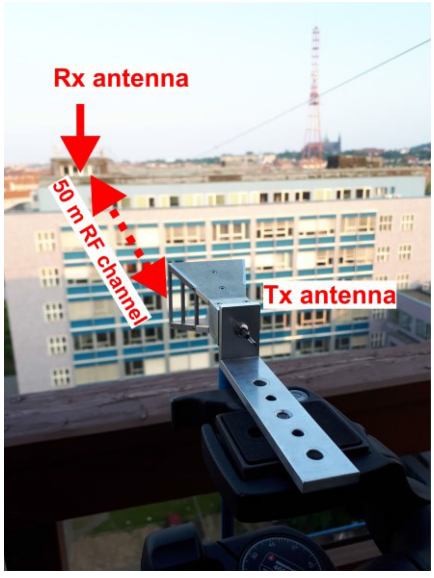

Fig. 3. 50-m long free-space RF channel with detail on the transmitting antenna (Tx).

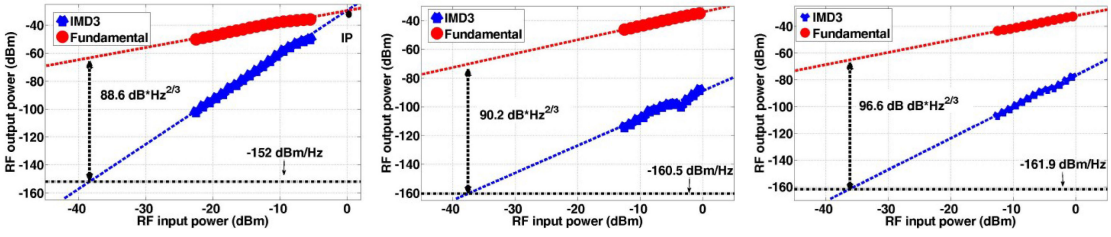

Fig. 4. System response (denoted as "Fundamental") and IMD3 for (a) Transmitter A (DML), (b) Transmitter B (EAM), and (c) Transmitter C (MZM). SFDR and IP are also shown.

Additionally, another measuring setup was built to characterize the free-space RF channel. The scheme consisted of the RF parts shown in Fig. 2 without any optics, i.e., it comprised signal generators with RF-MOD, a combination of Tx and Rx antennas, and two LNAs (Miteq AMF-4F-260400-40-10p and Analog devices HMC1131).The received signal was evaluated by the signal analyzer.

Our experimental work consisted of two subsequent experiments – a laboratory characterization of the RoF part, followed by the characterization of the entire RoF link with an outdoor free-space RF channel.

3. Indoor Experimental Results

Firstly, the linearity of the three transmitters (A, B, and C) using the laboratory setup (Fig. 1) was compared. Third-order intermodulation distortion (IMD3) was measured using a standard two-tone test with enabling the IMD3, spurious-free dynamic range (SFDR) and the third-order intercept point (IP3) to be evaluated. The results, measured at a frequency of 25 GHz with 1 MHz spacing between two tones, for all three transmitters using the same photodetector, are shown in Figs. 4a), b) and c).

SFDRs of 88.6, 90.2 and 96.6 dB·Hz$^{2/3}$ for Transmitters A, B and C, respectively, were obtained with corresponding input IP3s of 0, 50, and 31 dBm. Results show that Transmitter C had the lowest

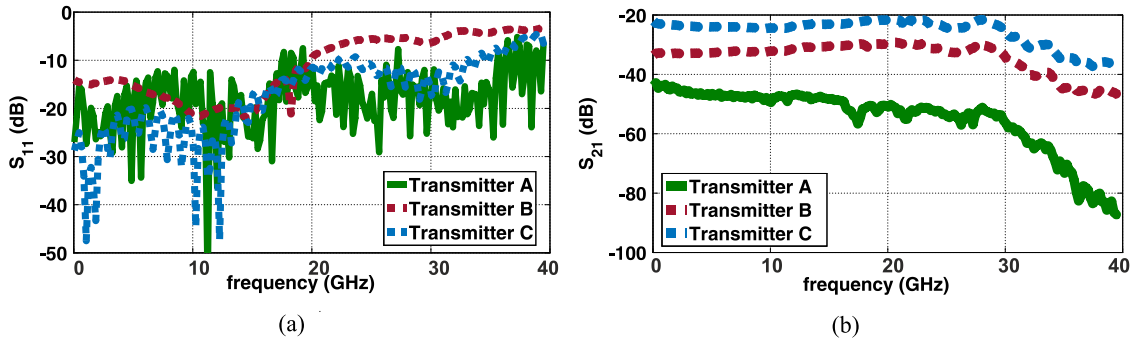

Fig. 5. (a) S_{11} and (b) S_{21} measured characteristics for Transmitters A (green solid line), B (red dotted line), and C (blue dashed line) in the frequency range 0–40 GHz.

third-order distortion (SFDR = 96.6 dB·Hz$^{2/3}$), followed by Transmitter B (SFDR = 90.2 dB·Hz$^{2/3}$). Transmitter A had the highest nonlinearity in terms of IMD3, mainly due to a considerably higher noise floor, but on the other hand, the input power did not exceed a critical value to generate significant nonlinear distortion. It is worth noting that the linearity measurement of Transmitter A was influenced by the bias-tee and especially by the additional RF amplifier that was necessary to boost RF power at its input to maintain the same power level as Transmitters B and C what resulted in the lowest linearity in terms of the SFDR. Transmitter B had the highest level of allowable input power in terms of IP3, i.e. 50 dBm. In the next step, S_{11} and S_{21} parameters for frequencies up to 40 GHz were measured using a vector network analyzer (R&S ZVA67). Measured data for all three transmitters are presented in Fig. 5. The vector measurement was carried out for an optical back-to-back setup without any other components, i.e., without the RF amplifier otherwise used with Transmitter A.

Note that S_{11} result of Transmitter A (Fig. 5a) involved the input matching load of the bias tee since the DML had no direct RF input and show an excellent matching with S_{11} mostly below -10 dB in bandwidth between 20 and 30 GHz. Transmitter B evinced at the input a very low impedance match of -5.5 dB in terms of S_{11} at 25 GHz compared to -11 dB and -16.5 dB for Transmitters A and C, respectively. Nevertheless, the results imply low frequency-dependent transmission in terms of S_{21} for all three transmitters with frequencies up to 30 GHz (Fig. 5b) showing a comparable course. Additionally, Transmitters B and C have an almost identical shape of S_{21} curves, suggesting the measured performance is predominantly given by the photodetector. The average S_{21} magnitude difference between Transmitters B and C was 7 dB, mainly caused by the modulation depth. The DML in Transmitter A was designed to operate over a wider frequency range of up to 40 GHz [26], however, its S_{21} performance was highly influenced by the frequency profile of the photodetector used and, in particular, by the bias tee. It resulted in a less flat characteristic compared to Transmitters B and C. The S_{21} measured at frequency of 25 GHz were -53.9, -32.3 and -24.2 dB for Transmitters A, B and C, respectively. Note that considerably lower transmission with Transmitter A was caused by the exclusion of an RF amplifier in front of its bias tee input. The IL, meaning the RF signal transfer to optical and back from optical to the RF domain, measured in an indoor scenario for a particular setup with parameters given in section II at a frequency of 25 GHz, was 32.4 dB (53.3 dB without an amplifier in front of the DML), followed by 38.9 dB and 30.2 dB for Transmitters A, B and C, respectively.

Furthermore, the RoF link performance without the free-space RF channel was analyzed in laboratory conditions. Its performance was first characterized in terms of EVM over a frequency range of 22.5 GHz to 26.5 GHz by using a 20 MHz LTE signal bandwidth and 16-QAM modulation from the test model TM 3.2. Results are then shown in Fig. 6. The highest received RF power and corresponding absolute lowest EVM of 2.3% in the selected frequency range were achieved with Transmitter C. The measured EVM values at 25 GHz were 3.7, 3.7 and 2.4% for Transmitters A, B and C, respectively, showing comparable performance of Transmitters A and B for indoor scenario.

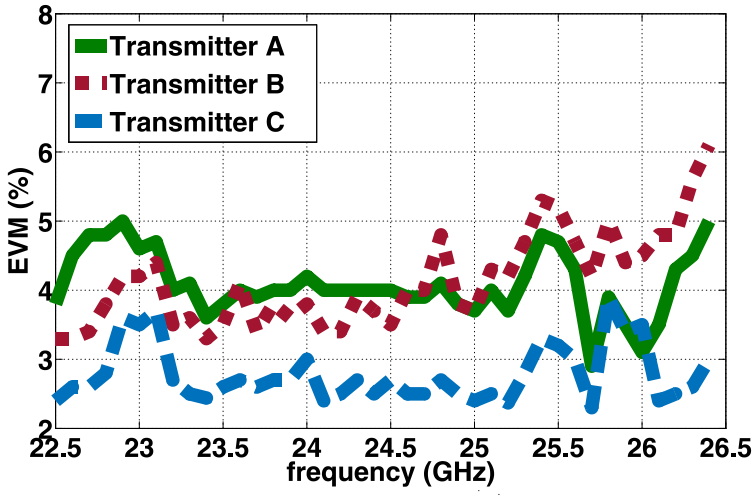

Fig. 6. Measured EVM for Transmitters A (green solid line), B (red dotted line), and C (blue dashed line) in the frequency range of 22.5 GHz–26.5 GHz in laboratory conditions.

The best EVM performance while using Transmitter C has been achieved especially due to the above mentioned high RF power transmission and low IMD3, which directly affects the signal in used bandwidth.

It can be observed that the profile of EVM for all transmitters partially follows the frequency response of the jointly-used equipment/components, which can be seen, e.g., at 23.1 or 25.8 GHz where all three curves evince similar peaks. However all performances in selected bandwidth keep under the EVM of 6%, which is greatly under the EVM limit for 16-QAM. In order to evaluate potential margins in the system power budget, we tested the resilience of the laboratory RoF setup to additional optical loss, which was introduced by using a VOA as depicted in Fig. 1. Measured results for indoor setup at 25 GHz are shown in Fig. 7. The black-dotted horizontal line indicates the 13.5% limit given by the 3GPP for the 16-QAM modulation scheme [30]. Constellation diagrams with EVM of 3.3, 3.7 and 2.4% for Transmitter A, B and C, respectively, are shown in Fig. 7b).

The maximum margins for additional optical losses were 9.2, 6.7, and 11.2 dB for Transmitters A, B, and C, respectively. In other perspectives, the EVM magnitudes were 6.5, 11.5 and 4.9% when setting the allowable margin to 6 dB to keep all scenarios with EVM under 13.5% and providing large margin for e.g. fiber length extension.

4. Outdoor Experimental Results

A large unlicensed bandwidth is provided by the mm-wave band between 24–28 GHz though significant challenges remain, in particular, high free-space propagation loss. As shown below, another limitation is introduced by significant power fluctuations due to perturbations in the atmosphere.

4.1. Free-space RF channel characterization

To characterize the free-space RF channel stability in RoF system, received RF power fluctuations were monitored by using both data and single-carrier transmission at the 25 GHz frequency described in Chapter II. For the sake of comparison, a single-carrier transmission at 5 GHz was also tested. Results from a one-hour measurement of the received LTE signal power fluctuation within test model TM 3.2, with 20 MHz bandwidth and 16-QAM modulation at 25 GHz, are shown in Fig. 8. Note that the data were taken each 100 ms to capture even fast signal fades. As can be seen, the signal experienced high power fluctuations around the mean power level of -45.7 dBm with a standard deviation of 1.9 dB, which follows the probability density function of normal distribution

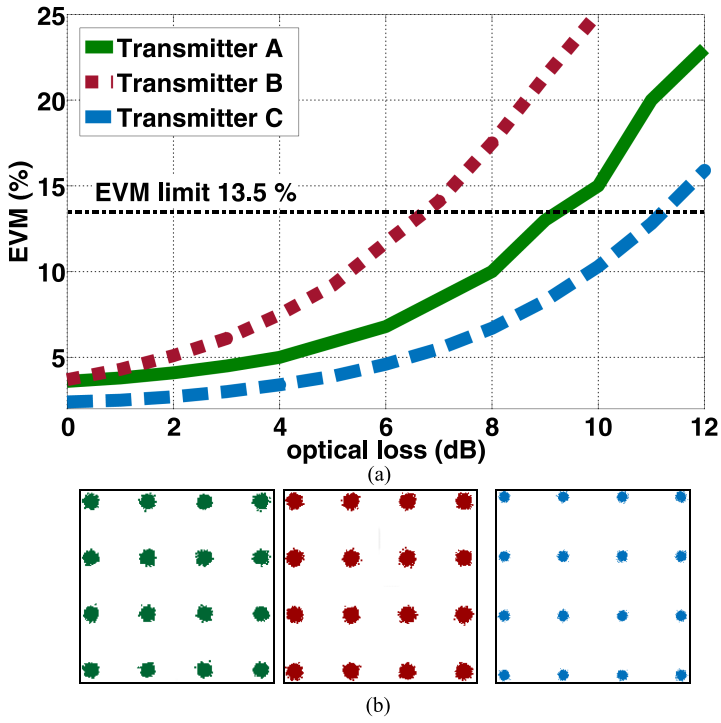

Fig. 7. (a) EVM vs. additional optical loss for indoor links with Transmitters A (green solid line), B (red dotted line), and C (blue dashed line) at a frequency of 25 GHz and (b) corresponding constellation diagrams for Transmitter A, B, and C with 16-QAM at 0 dB of optical attenuation.

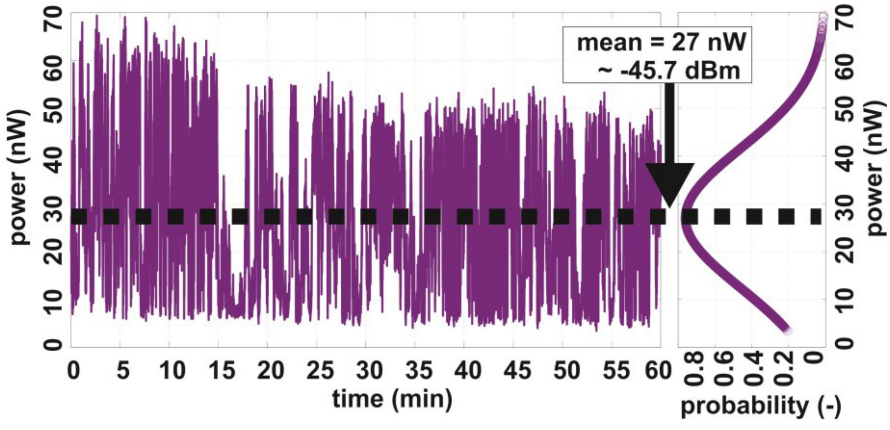

Fig. 8. Measured received power fluctuations following propagation through 50-m long free-space RF channel at a carrier frequency of 25 GHz with the 20 MHz bandwidth LTE data including the corresponding probability density function.

as depicted in the inset in Fig. 8. Note, this result is in line with calculations and measurements presented in the literature. For example, the experimental measurements and empirical-based propagation channel models at 28 GHz reported a standard deviation of 1.1 dB for the directional path loss model with line-of-sight [33].

Another study [34] presented data from a path loss model for usage within 5G in urban macrocells, microcells and indoor scenarios. The standard deviation of power fluctuation was modeled to be as large as 3.2 dB at 28 GHz for a distance range of 31–54 m [34]. Moreover, the free-space channel condition has been examined especially in terms of atmospheric effects

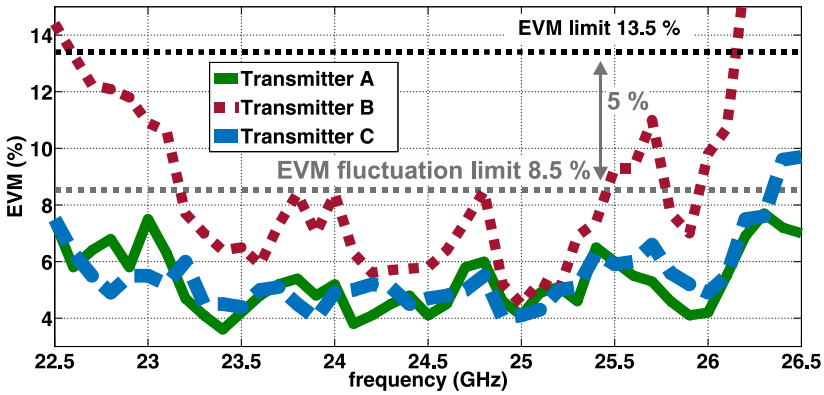

Fig. 9. Measured EVM for Transmitters A (green solid line), B (red dotted line), and C (blue dashed line) in the frequency range of 22.5–26.5 GHz for outdoor measurement.

that revealed a non-negligible correlation between received RF signal power with wind speed and consequently with air humidity, which was between 50–62% in given measuring interval. The magnitude of Pearson correlation coefficient of received RF power and humidity was 0.31 denoting weak correlation with the presence of the water particles in the air. To further gain insight into the measured power fluctuations, additional tests transmitting only a single-tone (instead of the LTE signal) were performed at 25 GHz. Power fluctuations in terms of a standard deviation of 2.3 dB were observed. When the single-tone signal frequency was decreased to 5 GHz, power fluctuations were reduced to 0.8 dB, making 1.5 dB difference compared to the 25 GHz frequency.

All our measurements were carried out during clear, sunny September days with similar conditions (temperatures around 14 °C). To confirm the achieved results, we repeated the measurement several times with comparable weather conditions and acquired similar results. As we did not observe any power fluctuations of such magnitude in our indoor experiment using the same hardware published earlier [27], we conclude that the fluctuations were caused exclusively by the atmospheric conditions.

Considering our experiments were carried out during clear days suggests that significantly stronger power fluctuations may be expected during harsh weather conditions. As the power fluctuations may significantly influence system performance (and especially power margins), weather conditions must be carefully considered and their influence on power fluctuations needs to be characterized when designing a free-space RF channel operating at the 25 GHz band.

4.2. Overall optical and RF system performance

In the final step, the whole system, including RoF and the outdoor free-space RF channel, was tested according to the indoor measurement campaign. The performance was again characterized in terms of EVM over a frequency range of 22.5 GHz to 26.5 GHz using a 20 MHz LTE signal bandwidth and test model TM 3.2 with 16-QAM modulation. Note that the EVM values were captured as a mean value according to received power fluctuations whose distribution is displayed in Fig. 8. Results from the EVM measurement are shown in Fig. 9. Due to the lower output optical power, the configuration of Transmitter A used an internal RF amplifier at the signal analyzer to obtain a similar level of detected signal power as that obtained with Transmitters B and C. As expected, the highest received power, as well as the lowest EVM in the selected frequency range, was achieved by Transmitter C with MZM like in indoor scenario. However, Transmitter A performed quite similarly to Transmitter C also thanks to activated additional RF amplifier in the receiver, which improved the signal power. We achieved a mean EVM below 6%, well below the limit of 13.5%, for all three transmitters at 25 GHz. However, Transmitter B only evinced an EVM under 13.5% over a reduced frequency range of 22.6–26.1 GHz. This is surprising as Transmitters A and C performed

sufficiently well over the entire spectral range studied, whereas optical power of Transmitter C was at the same level as for Transmitter B. We attribute the overall poorer performance of Transmitter B to its relatively lower ER and worse impedance matching and lower S_{21} transmission, as compared to Transmitters A and C. As concerns EVM values obtained for the outdoor setup, it was as low as 4.1% when using Transmitters A and C, and 4.5% when using Transmitter B at 25 GHz. This represents only a modest degradation when compared to the laboratory setup performance. The considered 4-GHz bandwidth is reduced, especially for Transmitter B on both edges of the considered spectrum. For all transmitters, the EVM increases above the frequency of approximately 25.2 GHz due to frequency-dependent losses, a small drop in S21 characteristics (see Fig. 5b) at this frequency and increased noise of the receiver, which steeply rises above 26 GHz and results in the degradation of SNR. We can also observe the increased EVM values for frequencies below 23.4 GHz for all transmitters because of the frequency-dependent gain of used amplifiers. The aforementioned reasons led to significantly increased EVM values for Transmitter B, having about 8 dB lower power transmission, about 6 dB worse impedance matching and 6.4 dB lower dynamic range compared to Transmitter C and whose different transmission parameters have become apparent in outdoor system usage. Moreover, the Transmitter B evinced the lowest SNR from all transmitters in outdoor scenario, namely 29.8 dB at 25 GHz. Whereas the SNR of the Transmitter B was lower by 3.5 and 2.2 dB at 25 GHz, comparing to the Transmitters A and C, respectively, the SNR at 24 GHz was lower by 5.5 and 6 dB, respectively and lower by 4.5 and 3.5 dB at the frequency of 26 GHz, comparing to the Transmitter A and C, respectively. Therefore the overall performance was more deteriorated in the edges of considered bandwidth for Transmitter B. Note that the displayed EVM figures are mean values. When taking power fluctuations into account, the EVM also fluctuated, with up to a maximal $\pm$5% variation for the test model used at the 20 MHz bandwidth and 16-QAM. The updated limit, providing enough margin and ensuring a fluctuating EVM below the original limit, is shown as the grey dashed horizontal line at EVM of 8.5%. Unfortunately, this reduces the useful bandwidth for Transmitter B from 23.2 GHz to 25.4 GHz and for Transmitter C from 22.5 to 26.3 GHz.

Finally, we analyzed the effect of additional optical losses using the same approach as described in Section III. Measured results of EVM dependence on optical loss for all three transmitters are depicted in Fig. 10. As can be seen, there is a smaller maximum margin for additional optical losses for the outdoor setup than for the laboratory setup without the free-space RF channel. The maximum observed difference was 3.6 dB for Transmitter C. The optical loss of the outdoor system can be increased up to 6.8, 4.2 and 7.6 dB for Transmitters A, B, and C, respectively while keeping mean EVM below 13.5%.

On the other hand, when maximum RF received power fluctuation induced in the free-space RF channel at 25 GHz was accounted for, the margin for additional optical losses was reduced to 4.0, 3.1 and 5.0 dB for Transmitters A, B and C, respectively. These values were obtained without the use of an optical amplifier whose use would significantly extend the power budget margin to provide, e.g., SSMF link extension. The higher margin for optical losses achieved with Transmitter C is due to high optical power when using MZM, the linear characteristic of the MZM, and its high ER as well as the high transmission in terms of S_{21}. Fig. 10b) depicts constellation diagrams while using particular Transmitter with 0 dB of optical attenuation with corresponding EVM values of 4.3, 4.6 and 3.9% for Transmitter A, B and C, respectively.

5. Discussion

In the conducted experiment, we have shown that all three transmitters exhibit satisfactory performance for deployment in real-world RoF systems. Achieved results are in agreement with commonly observed differences in the performance of particular modulation configurations and we have shown which parameters can highly affect such a RoF link including a real outdoor antenna link. Based on our results, the importance of high signal power transmission, i.e. around 30 dB of IL or better for passive RoF, over optical infrastructure in terms of S21 parameter and impedance

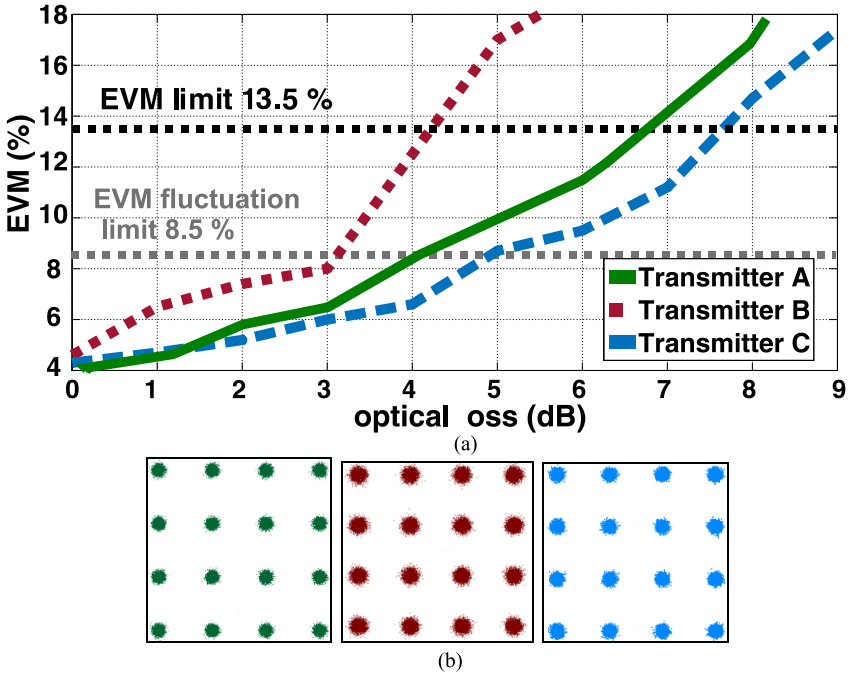

Fig. 10. EVM vs. additional optical losses when using Transmitters A (green solid line), B (red dotted line), and C (blue dashed line) at a frequency of 25 GHz in the outdoor setup and (b) corresponding constellation diagrams for Transmitter A, B, and C with 16-QAM at 0 dB of optical attenuation.

matching over a large frequency range can be clearly highlighted. Higher ER and immunity to IMD3 influencing the quality of the signal are also vital.

Apart from the above-mentioned observations, which may be straightforward for researchers in the RoF field, we examined real outdoor free-space RF link and we found that signal fluctuations affect the RoF system performance severely. Captured data analysis provided a nice insight into the channel behavior and proved to have the most significant effect on the overall RoF system. The main outcome is that even in a clear, sunny day, strong signal fluctuations of over 2-3 dB are present at 25 GHz, whereas lower frequencies are more resilient. Therefore, for RoF system analyses including antennas, it is important to measure in real conditions instead of laboratory verifications or at least to include the channel behavior based on published empirical data.

The delivery of sufficient RF power to the antenna depends, amongst others, also on the optical transmitter power and therefore we have added an additional RF amplifier in the RF receiver when using Transmitter A. Interestingly, with this additional RF amplifier, the RoF system performance was as good as with Transmitter C. Moreover, we demonstrated in [27] the excellent system performance under laboratory conditions with identical DML when the optical power was 3 dB higher and EDFA has been adopted to compensate the low DML output power. Based on the results, it is worth mentioning that the most appropriate approach for a specific solution needs to be considered in the context of other parameters like cost, size or integrability, which favours DML approach, even in the frequency band between 20 and 30 GHz.

The optical link serves here as a medium for radio signal transmission over longer distances than would be possible to reach with RF cable or antenna and therefore, margin for additional losses have been tested for both indoor and outdoor link and all presented approaches can be used with some limitations according to their particular parameters. Moreover, the complete RoF system including the RF wireless transmission at the frequency around 25 GHz needs more used RF components, namely RF amplifiers to compensate high atmospherical attenuation in this band and high losses due to antenna broadcasting (note that in our case the RF free space losses

including antenna gain were 65 dB over 50 m distance because the used antenna has relatively wide radiating beam $> 30°$). Thus there is a number of RF amplifiers, which are necessary to get sufficient RF power budget. This considerably affects the overall system performance by the uneven amplifier gain in the given bandwidth and also noise floor increases.

In our study, we used a lower data rate (TM 3.2 LTE test model with 20 MHz bandwidth and 16-QAM modulation scheme), nevertheless, the achieved results suggest the system has the potential to operate even at 100 MHz bandwidth or more. This we demonstrated in [27] for an indoor-only based system where we achieved 375 Mb/s throughput with the same DML as we used in this study for Transmitter A.

6. Conclusions

We have demonstrated an experimental RoF transmission of mm-wave signal with a 50-meter long outdoor free-space RF channel in the frequency band of 25 GHz. The best system performance has been achieved by using Transmitter A (based on a DML) and Transmitter C (based on MZM). In the outdoor scenario, the mean EVM for the aforementioned transmitters was below 8.5% over the entire tested 4 GHz bandwidth window, giving reasonable margin for the 16-QAM requirement of $<$13.5% EVM, budgeting for the expected power variations due to the received power fluctuations in the free-space RF channel. The Transmitter A compared to Transmitter C is potentially significantly cheaper, simpler, and more compact, making it a better candidate for large-scale deployment, e.g., in 5G networks. Moreover, we have shown that the lower output optical power in the case of Transmitter A can be compensated by additional RF amplifier in the receiver and therefore equalize the Transmitter C with MZM. Transmitter B (based on EAM) achieved adequate overall EVM performance but with degradation towards both edges of the spectral band studied in the outdoor experiment. The EAM performance suffers from an achieved trade-off between satisfactorily high ER (i.e., 15 dB vs. 20 dB with MZM) and acceptable IL, lower linearity, RF transmission and impedance matching when compared to Transmitter C what led in real outdoor system with additional RF equipment to considerable signal fading. However, Transmitters A and B represent an integrated and, thus, potentially low cost and compact solution. Furthermore, we characterized all three transmitters in the RoF channel to evaluate potential margins in the system power budget. All of them can provide more than 3 dB (Transmitter C up to 6 dB) when considering maximal EVM variation due to a wireless transmission at 25 GHz. Finally, we reported on a significant signal power fluctuation for the free-space RF channel at 25 GHz, whose impact needs to be taken into account (e.g., considering higher power margins) when designing such a link. The standard deviation of received power, while using a 16-QAM transmission with a 20 MHz bandwidth at 25 GHz over a 50-m long wireless channel, was 1.9 dB resulting in maximal EVM variation of $\pm$5%.

References

[1] S. Mattisson, "Overview of 5G requirements and future wireless networks," in *Proc. 43rd IEEE Eur. Solid State Circuits Conf.*, 2017, pp. 1–6.
[2] T. S. Rappaport *et al.*, "Millimeter wave mobile communications for 5G cellular: It will work!," *IEEE Access*, vol. 1, pp. 335–349, 2013.
[3] B. Lannoo *et al.*, "Radio-over-fibre for ultra-small 5G cells," *Proc. 17th Int. Conf. Transparent Opt. Networks*, 2015, pp. 1–4.
[4] P. T. Dat, A. Kanno, and T. Kawanishi, "Radio-on-radio-over-fiber: efficient fronthauling for small cells and moving cells," *IEEE Wirel. Commun.*, vol. 22, no. 5, pp. 67–75, Oct. 2015.
[5] P. J. Urban, G. C. Amaral, and J. P. Von Der Weid, "Fiber monitoring using a sub-carrier band in a sub-carrier multiplexed radio-over-fiber transmission system for applications in analog mobile fronthaul," *J. Lightw. Technol.*, vol. 34, no. 13, pp. 3118–3125, 2016.
[6] C. H. Lee, *Microwave Photonics*, 2nd ed., New York, NY, USA: Taylor & Francis, 2013.
[7] T. Kanesan, W. P. Ng, Z. Ghassemlooy, and C. Lu, "Experimental demonstration of the compensation of nonlinear propagation in a LTE RoF system with a directly modulated laser," in *Proc. IEEE Int. Conf. Commun.*, 2013, pp. 3884–3888.
[8] D. Novak *et al.*, "Radio-over-fiber technologies for emerging wireless systems," *IEEE J. Quantum Electron.*, vol. 52, no. 1, pp. 1–11, Jan. 2016.

[9] U. Habib, M. Steeg, A. Stöhr, and N. J Gomes, "Radio-over-fiber-supported 60 GHz multiuser transmission using leaky wave antenna," in *Proc. Int. Topical Meeting Microw. Photon.*, 2017, pp. 1–4.
[10] J. Beas, G. Castanon, I. Aldaya, A. Aragon-Zavala, and G. Campuzano, "Millimeter-wave frequency radio over fiber systems: A survey," *IEEE Commun. Surv.*, vol. 15, no. 4, pp. 1593–1619, Oct. –Dec. 2013.
[11] T. Yeyu, C. Chow, G. Chen, C. Peng, C. Yeh, and H. Tsang, "Integrated silicon photonics remote radio frontend (RRF) for single-sideband (SSB) millimeter-wave radio-over-fiber (ROF) systems," *IEEE Photon. J.*, vol. 11, no. 2, Apr. 2019, Art. no. 7202108.
[12] D.-N. Nguyen *et al.*, "M-QAM transmission over hybrid microwave photonic links at the K-band," *Opt. Express*, vol. 27, pp. 33745–33756, 2019.
[13] L. Vallejo, B. Ortega, J. Bohata, S. Zvanovec, and V. Almenar, "Photonic multiple millimeter wave signal generation and distribution over reconfigurable hybrid SSMF/FSO links," *Opt. Fiber Technol.*, vol. 54, 2020, Art. no. 102085.
[14] H. Li *et al.*, "Real-time 100-GS/s sigma-delta all-digital radio-over-fiber transmitter for 22.75–27.5 GHz band," in *Proc. Opt. Fiber Commun. Conf. Exhib*, 2019, pp. 1–3.
[15] S. H. Lee, H. J. Kim, and J.I. Song, "Simultaneous multichannel photonic frequency up-conversion based on an EAM and an optical interleaver for radio-over-fiber systems," in *Proc. IEEE Int. Topical Meeting Microw. Photon.*, 2012, pp. 220–223.
[16] S. A. Khwandah, J. P. Cosmas, I. A. Glover, P. I. Lazaridis, N. R. Prasad, and Z. D. Zaharis, "Direct and external intensity modulation in OFDM RoF links," *IEEE Photon. J.*, vol. 7, no. 4, Aug. 2015Art. no. 7902710.
[17] D. Wake *et al.*, "A comparison of radio over fiber link types for the support of wideband radio channels," *J. Lightw. Technol.*, vol. 28, no. 16, pp. 2416–2422, Aug. 2010.
[18] A. Lebedev, X. Pang, J. J. V. Olmos, S. Forchhammer, and I. T. Monroy, "Simultaneous 60-GHz RoF transmission of lightwaves emitted by ECL, DFB, and VCSEL," *IEEE Photon. Technol. Lett.*, vol. 26, no. 7, pp. 733–736, Apr. 2014.
[19] Z. Tang, J. Zhang, S. Pan, G. Roelkens, and D. Van Thourhout, "RoF system based on an III-V-on-silicon transceiver with a transfer-printed PD," *IEEE Photon. Technol. Lett.*, vol. 31, no. 13, pp. 1045–1048, Jul. 2019.
[20] K. V. Gasse *et al.*, "480 Mbps/1 Gbps radio-over-fiber link based on a directly modulated III-V-on-Silicon DFB laser," in *Proc. IEEE Int. Topical Meeting Microw. Photon.*, 2016, pp. 328–331.
[21] E. Martin *et al.*, "28 GHz 5G radio over fibre using UF-OFDM with optical heterodyning," in *Proc. IEEE Int. Topical Meeting Microw. Photon.*, 2017, pp. 1–4.
[22] A. Naemat, S. M. Mohd Hassan, N. F. I. Muhammad, A. S. M. Marzuki, and N. Kushairi, "Experimental study on LTE signal transmission in multi-service Radio-over-Fiber (RoF) system," in *Proc. IEEE 13th Malaysia Int. Conf. Commun.*, 2017, pp. 300–304.
[23] U. Habib, A. E. Aighobahi, C. Wang, and N. J. Gomes, "Radio over fiber transport of mm-wave 2×2 MIMO for spatial diversity and multiplexing," in *Proc. IEEE Int. Topical Meeting Microw. Photon.*, 2016, pp. 39–42.
[24] S.E. Alavi, M. R. K. Soltanian, I. S. Amiri, M. Khalily, A. S. M. Supa'at, and H. Ahmad, "Towards 5G: A photonic based millimeter wave signal generation for applying in 5G access fronthaul," *Sci. Rep.*, vol. 6, 2016, Art. no. 19891.
[25] O. Alkhalifah, O. Alrabiah, A. Ragheb, M. A. Esmail, and S. Alshebeili, "Investigation and demonstration of 5G signal transmission over fiber/FSO/wireless links," in *Proc. Int. Conf. Elect. Comput. Technologies Appl.*, 2017, pp. 1–4.
[26] M. A. Esmail, A. M. Ragheb, H. A. Fathallah, M. Altamimi, and S. A. Alshebeili, "5G-28 GHz signal transmission over hybrid all-optical FSO/RF link in dusty weather conditions," *IEEE Access*, vol. 7, pp. 24404–24410, 2019.
[27] J. Bohata, J. Spáčil, Z. Ghassemlooy, S. Zvánovec and R. Slavík, "24-26 GHz radio-over-fiber and free-space optics for fifth-generation systems," *Opt. Lett.*, vol. 43, no. 5, pp. 1035–1038, 2018.
[28] A. Stohr *et al.*, "Millimeter-wave photonic components for broadband wireless systems," *IEEE Trans. Microw. Theory Techn.*, vol. 58, no. 11, pp. 3071–3082, Nov. 2010.
[29] S. Rommel *et al.*, "225 m Outdoor W-band radio-over-fiber link using an optical SFP+ module," in *Proc. Opt. Fiber Commun. Conf. Exhib.*, 2016, pp. 1–3.
[30] The 3rd Generation Partnership Project. [Online]. Available: www.3gpp.org
[31] J. Kreissl, V. Vercesi, U. Troppenz, T. Gaertner, W. Wenisch, and M. Schell, "Up to 40-Gb/s Directly modulated laser operating at low driving current: buried-heterostructure passive feedback laser (BH-PFL)," *IEEE Photon. Technol. Lett.*, vol. 24, no. 5, pp. 362–364, Mar. 2012.
[32] J. Bohata, J. Spacil, S. Zvanovec, Z. Ghassemlooy, and R. Slavik, "Hybrid RoF-RoFSO system using directly modulated laser for 24–26 GHz 5G Networks," in *Proc. 11th Int. Symp. Commun. Syst., Networks Dig. Signal Process.*, 2018, pp. 1–5.
[33] T. S. Rappaport, G. R. MacCartney, M. K. Samimi, and S. Sun, "Wideband millimeter-wave propagation measurements and channel models for future wireless communication system design," *IEEE Trans. Commun.*, vol. 63, no. 9, pp. 3029–3056, Sep. 2015.
[34] S. Sun *et al.*, "Investigation of prediction accuracy, sensitivity, and parameter stability of large-scale propagation path loss models for 5G wireless communications," *IEEE Trans. Veh. Technol.*, vol. 65, no. 5, pp. 2843–2860, May 2016.